OPEN

RETINAL DISPLACEMENT AFTER IDIOPATHIC MACULAR HOLE SURGERY

Layer by Layer Analysis

TOMMASO ROSSI, MD,* GIORGIO QUERZOLI, PHD,† GUIDO RIPANDELLI, MD,* LUCA PLACENTINO, MD,* MARIACRISTINA PARRAVANO, MD,* DAVID H. STEEL, MD,‡ MARIO R. ROMANO, MD, PHD§

Purpose: To measure the displacement of retinal vascular *plexi* and choriocapillaris after pars plana vitrectomy for idiopathic macular hole, using optical coherence tomography angiography, and correlate it with clinical data.

Methods: Retrospective series with a 6-month follow-up. Records included Best Corrected Visual Acuity, M-charts, structural optical coherence tomography, and optical coherence tomography angiography. Coronal displacement was calculated comparing consecutive images across the 6.4 mm × 6.4 mm field and concentric circular regions of 0.5, 1.5, and 3.0 mm *radii*. Each circular region was further divided in four quadrants indicated as follows: SuperoTemporal; SuperNasal; InferoTemporal; InferoNasal.

Results: The study comprised 33 patients (11 men and 22 women) with 68.9 ± 10.2 years mean age, similar among sexes. Macular hole closed in 31/33 (93.9%) of cases and Best Corrected Visual Acuity improved from mean 20/62 (0.50 ± 0.62 logarithm of Minimum Angle of Resolution) to 20/47 (0.23 ± 0.63 logarithm of Minimum Angle of Resolution; $P = 0.0064$). Vertical and horizontal metamorphopsia decreased from 0.98 ± 0.68 to 0.51 ± 0.59° ($P = 0.0028$) and 0.84 ± 0.63 to 0.29 ± 0.45° ($P < 0.001$), respectively. The average retinal displacement was 81.2 ± 44.1 μm for the superficial *plexus* and 79.4 ± 45.7 μm for the deep one, both greater than the choriocapillaris displacement (60.9 ± 20.2 μm; $P < 0.05$). The temporal and superior quadrants displaced more than the others ($P < 0.05$). Macular hole size correlated to retinal displacement within the central 0.5-mm radius area at all layers ($P < 0.05$ in all cases).

Conclusion: Macular hole closure is associated with significant retinal displacement of all retinal layers and choriocapillaris remodeling. Surgical peeling removes the constraining effect of the internal limiting membrane and promotes a multilayered displacement that fills the retinal defect, likely due to a change in the equilibrium of forces between the contractile retinal structures: the larger superficial retinal vessels and the retinal nerve fiber layer.

RETINA 45:410–419, 2025

Full-thickness idiopathic macular holes (IMH) result from a dehiscence of all retinal layers at the fovea, whose pathogenesis has been related to the contraction of vitreous cortex remnants, eventually leading to tissue disruption.[1,2] Idiopathic MHs have also been described after vitreous removal[3] while traumatic MHs are thought to result from the propagation and reflection of pressure waves.[4]

Pars plana vitrectomy (PPV) with or without internal limiting membrane (ILM) peeling or inverted flap[5] represents the treatment of choice with over 85% reported anatomic success,[6] although the spontaneous closure of IMHs is a rare but well-known event.[7] The mechanism underlying IMH closure after PPV has been debated but is mostly attributed to the surgical release of tangential (i.e., coronal) vitreous cortex tractions over the foveola and the reduction of inner retinal layer stiffness after ILM peeling.[8] The pooling of growth factors within the foveal microenvironment created by ILM flaps has also been hypothesized[9] and IMH closure patterns systemically classified.[10]

We recently introduced a procedure to measure retinal displacement based on image processing[11] and used it to describe the retinal displacements occurring before and after macular pucker surgery,[12] using both infrared and optical coherence tomography (OCT).

Optical coherence tomography angiography (OCTA) is a robust, well-accepted diagnostic tool capable of identifying flow and imaging the retinal vascular *plexi*[13] separately. The purpose of this study was to calculate the retinal displacement after successful PPV for IMH, using OCTA images of the choriocapillaris, deep, and superficial vascular *plexi*, to evaluate their pattern of deformation and thus the contribution of each layer to the repair mechanism.

Materials and Methods

Study Participants

We retrospectively analyzed the records and OCT images of all patients operated with PPV and an inverted ILM flap for IMH by a single surgeon with postoperative follow-up longer than 6 months. All patients received surgery at the IRCCS Bietti Foundation between October 2022 and June 2023.

Exclusion criteria were as follows: (1) concomitant history of ocular and specifically macular disorders including age-related macular degeneration, retinal vascular occlusions, retinal detachment, trauma, ametropias exceeding sf +1 and sf −3 diopters in spherical equivalent refraction, and uveitis; (2) history of systemic diseases, including hypertension and diabetes; (3) poor imaging quality due to media opacity; (4) incomplete medical records; and (5) diagnosis of macular hole (MH) for more than 6 months.

All patients had at least three complete ophthalmic assessments after surgery, with manifest and corrected refraction, Best Corrected Visual Acuity (BCVA) using Early Treatment Diabetic Retinopathy Study acuity charts converted to the logarithm of Minimum Angle of Resolution units for statistical purposes. The degree of horizontal and vertical metamorphopsia was assessed through M-CHARTS (Inami, Co, Tokyo, Japan).[14] All included patients had the above information available just before the intervention (T_0) and 1, 3, 6, months (±7 days) after surgery (hereafter indicated by T_1, T_3, and T_6, respectively). Included patients had a full thickness MH, according to the international committed classification.[15]

All patients provided written informed consent; the study adhered to the tenets of the Declaration of Helsinki and received approval of the local Ethics Committee (ERMLAB01 N° 77/18/FB).

Surgical Procedure

All patients underwent a standard 25-gauge three-port PPV with combined uneventful phacoemulsification and intraocular lens placement in the capsular bag, if phakic (using BVI R-Evolution CR800; BVI Medical Waltham, MA). All patients underwent 360° ILM peeling and ILM inverted flap after a single Brilliant Blue G staining applied before attempting ILM peeling manoeuvres (Monoblue, BVI Medical Waltham, MA), aiming at creating a round 360° "classic" ILM flap spanning the vascular arcades. All patients have been left with air in the vitreous chamber at the end of the procedure, making sure that the ILM flap fell on the MH at the end of the fluid–air exchange.

Optical Coherence Tomography Image Acquisition

Spectral domain OCT (Optovue Solix; Optovue Inc - Fremont CA) images were acquired using a horizontal SD-OCT cross-sectional scanning protocol.

Optical coherence tomography angiography images were also acquired at each visit and automatic segmentation for the choroidal, deep retinal, and superficial retinal *plexi* used. *En-face* OCT scans at the ILM level were also used to trace the ILM peeling border. Only patients whose scans were performed enabling the follow-up mode were included in the study to ensure repeatability.

Coronal Displacement Measures

Coronal displacement was measured by comparing the displacement occurring between two successive OCTA images, as previously described.[4] This study compared the first month after surgery (T_0–T_1), the following three months (T_1–T_3) (post-operative) and the entire course of the follow-up (T_0–T_6).

Coronal displacement measures used OCTA images, 6.4 mm × 6.4 mm in size, obtained during each visit under follow-up mode. As described in detail elsewhere,[4] the local anatomical structures visible on the digital images were compared to measure their displacements between the first and the second image using the Farneback motion estimation method. The algorithm approximates the images by means of polynomial functions and iteratively

From the *IRCCS - Fondazione Bietti ONLUS, Rome, Italy; †DICAAR – Università di Cagliari, Cagliari, Italy; ‡Biosciences Institute, Newcastle University, Newcastle Upon Tyne, United Kingdom; and §Department of Biomedical Science, Humanitas University, Milan, Italy.

None of the authors has any financial/conflicting interests to disclose.

Reprint requests: Tommaso Rossi, MD, IRCCS, Fondazione Bietti ONLUS, Via Livenza 3, Rome, 00198, Italy; e-mail: tommaso.rossi@usa.net

searches for the best displacement by minimizing the sum of squared differences between the predicted and actual local image intensities. In the first step, a rigid roto-translation minimizing the sum of the squared differences of the displacements yielded by the Farneback algorithm is subtracted to the second image at the aim of eliminating the unperfect alignment between the successive scans. In the successive step, the same algorithm was applied to the resulting images thus estimating the retinal deformation.

As a result of the procedure, the two components (*Dx*, horizontal, and *Dy*, vertical) of the displacement in the reference frame of the images were obtained in microns (as given by the OCT image scale) and mean values were computed using the magnitude of the local displacement vectors $D = \sqrt{Dx^2 + Dy^2}$ included in the selected region of interest.

Main Outcome Measures

Main study outcome measures included BCVA, M-Chart grading, central minimum foveal thickness, and mean retinal displacement of OCTA images.

Statistical Analysis

Analysis of variance with *t*-test and *t*-test for repeated measures applied to numerical variables were used to assess changes at different time points. Bivariate Pearson r correlation coefficient was applied for continuous variables, while Spearman rho and Kendall Tau were used for the assessment of ordinal variables. The Shapiro-Wilk test was used to assess normality. In all cases, *P* values <0.05 were considered statistically significant.

Results

Demographics, Visual Acuity, and Metamorphopsia

Overall, 33 patients (11 men and 22 women) satisfied the inclusion criteria; mean age was 68.9 ± 10.2 years, with no significant difference among sexes: 68 ± 11 years for women and 69.4 ± 8.5 for men. Seven patients were pseudophakic at T_0, the remaining were made pseudophakic at the time of surgery and underwent a combined PPV and uneventful phacoemulsification with intraocular lens implantation within the capsular bag.

Macular hole diameter on presentation was less than 250 μm in 6/33 eyes (18.1%), between 250 and 400 μm in 8/33 (24.2%) eyes, and greater than 400 μm in 19/33 (57.5%).

The MH closed in 31 cases (93.9%) and BCVA significantly improved from T_0 to T_1 (0.50 ± 0.62 logarithm of Minimum Angle of Resolution [20/62 Snellen] to 0.23 ± 0.63 logarithm of Minimum Angle of Resolution [20/47 Snellen]; $P = 0.0064$)) and showed a further trend toward improvement, although not significant, up to 6 months post-op. The 2 MHs that did not close belonged (one each) to the intermediate and bigger diameter class and the closure rate among diameter classes did not vary significantly.

Both vertical and horizontal metamorphopsia decreased significantly between T_0 and T_6 ($P = 0.0028$) from 0.98 ± 0.68 to 0.51 ± 0.59° and 0.84 ± 0.63 to 0.29 ± 0.45° ($P < 0.001$), respectively. There was no correlation between BCVA gain and metamorphopsia reduction.

Coronal (En-Face) Retinal Displacement

The average retinal displacement across the coronal plane throughout the 6 months follow-up is reported in Table 1 for each considered layer.

The choriocapillaris layer showed an average 60.9 ± 20.2 μm displacement, mostly located within the central 0.5 mm and displaced significantly less than the deep (79.4 ± 45.7 μm; $P < 0.05$) and superficial layers (81.2 ± 44.1 μm; $P < 0.05$; see also Table 1 and Figure 1). There was no significant displacement difference between the deep and superficial layers for any considered region.

The 2 MHs that did not close showed an average displacement of 40.82 ± 23.74 μm over the entire 6.4 × 6.4 mm analyzed superficial plexus, 49.50 ± 30.99 μm within the deep plexus, and 37.81 ± 29.03 μm of the choriocapillaris (the difference compared with successfully closed MHs was not significant).

Retinal displacement occurred mostly within the central circular region 0.5 mm in *radius* and was significantly greater than within the central region of 3-mm *radius* (see Table 2; $P < 0.05$). The displacement behavior over time is shown in Figure 2: all layers and considered regions showed a significantly higher displacement within the first month ($P < 0.01$ for all) compared with the following period.

The supero-temporal deep and superficial retinal *plexi* quadrant displaced more than any other quadrant (Figure 3; $P < 0.05$) within the central 1.5-mm *radius*, while the temporal choriocapillaris hemifield displaced more than all other choriocapillaris fields but less than the retinal *plexi* (Figure 4; $P < 0.05$ in all cases).

There was a significant correlation between MH size and retinal displacement across the different layers that have been reported in Table 2. There was no

Table 1. Retinal Displacement of all Vascular Layers (Mean ± SD; μm) Across the Coronal (*en-face*) Plane

Retinal Region	Choriocapillaris	Deep	Superficial
Entire image 6.4 × 6.4 mm	60.9 ± 20.2	79.4 ± 45.7	81.2 ± 44.1
R < 0.50 mm	66.4 ± 33.3	105.7 ± 41.2	110.8 ± 40.9
R < 1.50 mm	54 ± 39.3	84.2 ± 42.7	99.4 ± 48.3
R < 3.00 mm	56 ± 40.6	76.3 ± 42.4	81.4 ± 44.6

The entire scanned area was 6.4 × 6.4 mm wide and concentric rings at 0.50 mm, 1.50 mm, and 3.0 mm *radii* were also separately analyzed.

correlation between displacement at any level and metamorphopsia changes.

Discussion

Macular hole closure is a well-documented spontaneous or iatrogenic event, characterized by the rearrangement of retinal tissue across all retinal layers and associated with changes in the choriocapillaris.[16]

We used a method previously applied to retinal images[11 12], capable of tracing retinal displacement, to analyze MHs pre- and postoperative OCTA images and monitor the displacement of the superficial and deep retinal vascular *plexi* and the choriocapillaris. The superficial *plexus*, in fact, is positioned within the Ganglion Cell Layer and the deep capillary plexus below the Inner Nuclear Layer,[17] while the choriocapillaris does not belong to the retina and is located underneath the retinal pigment epithelium.[18]

The success rate, BCVA, and metamorphopsia improvement observed in this study was comparable to the existing literature, suggesting that this series does not differ from previously reported ones.[19]

Our data support the hypothesis that the entire 6.4 × 6.4-mm central retinal field and choriocapillaris contributed (or reacted) to MH closure, with an average displacement of about 75 μm (see Table 1 and Figure 1). Both retinal *plexi* (superficial and deep) displaced significantly more than the choriocapillaris and most displacement occurred within the first month (Figure 2) at all layers and tested eccentricity.

Interestingly, the choriocapillaris displaced significantly within the central 0.5-mm radius area, a process suggestive of vascular remodeling secondary to the metabolic changes imposed by the overlying retinal shift[20]; despite from the "tectonic" point of view, there is no void to fill at this level. On the other hand, an increase of choriocapillaris vascular density after MH repair has been previously reported.[21]

Topographically, the supero-temporal and supero-nasal quadrants displaced more than the others, across the central deep and superficial retinal *plexi*, while the choriocapillaris behaved somehow differently, with the supero-temporal and infero-temporal central quadrants (0.5-mm radius; Figure 3) exhibiting the maximum displacement. Consequently, the superior deep and superficial retinal hemifield shifted more intensely, while the temporal choriocapillaris hemifield displaced the most (Figure 4). Takeyama et al[22] also noticed a correlation between retinal displacement and inner

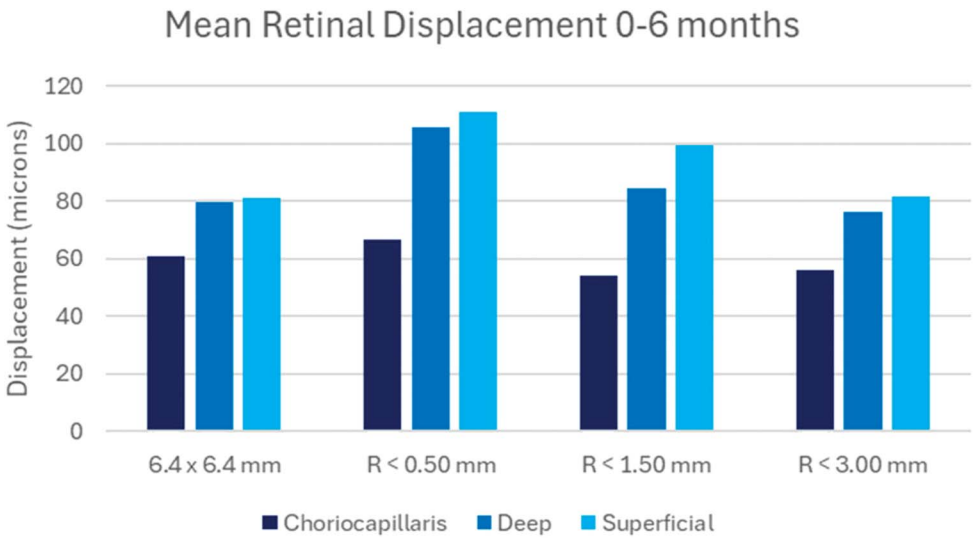

Fig. 1. Mean retinal displacement at all studied vascular layers between months T0 and T6 of follow-up.

Table 2. Linear Correlation Between MH Diameters and the Average Displacement Over the Circular Regions of all Tested *plexi*, Within the Central 0.5 mm and 1.5 mm *radius* From the Foveola

Retinal Region	Basal Hole Horizontal Diameter	Minimum Hole Horizontal Diameter
Choriocapillaris radius 0.5 mm	**0.040**	**0.029**
Choriocapillaris radius 1.5 mm	**0.013**	**0.002**
Deep radius 0.5 mm	**0.033**	**0.049**
Deep radius 1.5 mm	0.070	**0.023**
Superficial radius 0.5 mm	0.069	0.085
Superficial radius 1.5 mm	0.070	0.023

Pearson correlation values $P < 0.05$ are printed in bold.

nuclear layer thickness of the superior and temporal quadrants.

Previous studies already focused on retinal tectonics after successful MH surgery: Ishida et al[23] traced the linear distance between the optic nerve and vascular landmarks and noticed that the temporal retina displaced the most. In agreement with the present findings, they found a correlation between MH diameter and amount of displacement (Table 2) and that it mostly occurred within the first 2 weeks. After surgery, the retina tends to displace in proportion to the MH size until the entire MH width is spanned. The exact signaling mechanism of this intriguing process remains matter of speculation.

In addition, we noted that the two MHs that did not close showed less displacement compared with those that successfully closed, despite having similar MH size and areas of ILM peeling (Figure 5). Although the difference was not statistically significant, that is likely due more to the small sample size rather than the extent of displacement. The reason why some MHs exhibit less displacement than others, following otherwise identical surgical procedures, remains uncertain.

The pattern of maximum retinal displacement always occurred within the ILM peeling area (Figure 6, A–C) but rarely reached its boundaries, instead it seemed conditioned by the superficial *plexus* vessels path. It should be noted that the retina is a highly anisotropic and inhomogeneous structure,[24] whose mechanical properties, are determined by its stiffer structures such as the retinal vessels, due to their muscular wall. It is therefore conceivable that peeling manoeuvres favor and/or initiate retinal displacement by disrupting the integrity of the ILM, which is a physical constraint, but then the larger vessels "guide" displacement extension and orientation. The displacement shown in Figure 6, A–C, skims the vascular arcade and does not go any further, despite the ILM peeling extends more peripherally, as if indeed the vascular backbone influenced its deployment and prevented further extension. It has been reported that ILM peeling greater dimension facilitates MH closure[25] and seems also correlated with better visual outcome.[26]

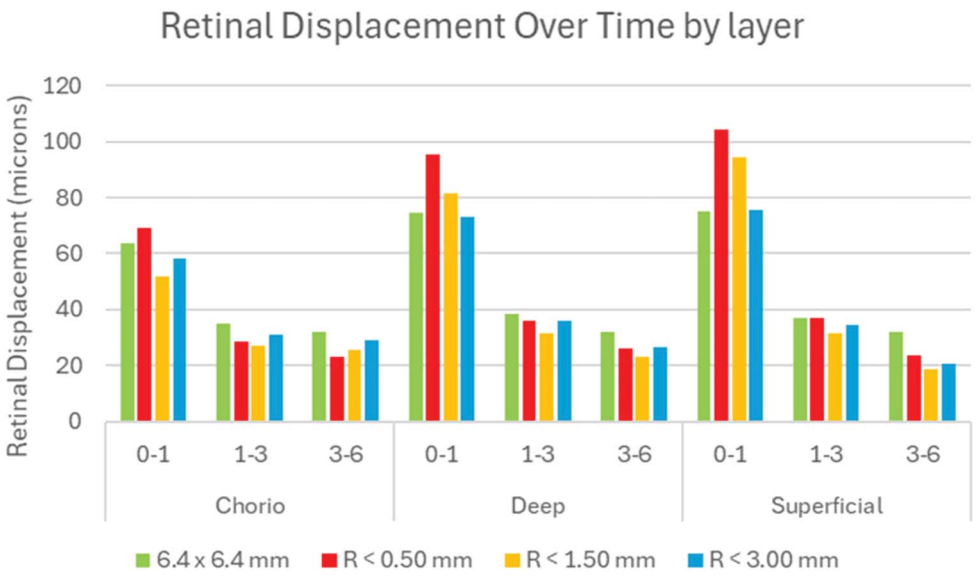

Fig. 2. Retinal displacement (in μm) over the follow-up period. All layers showed a significantly greater displacement within the first month compared with afterward.

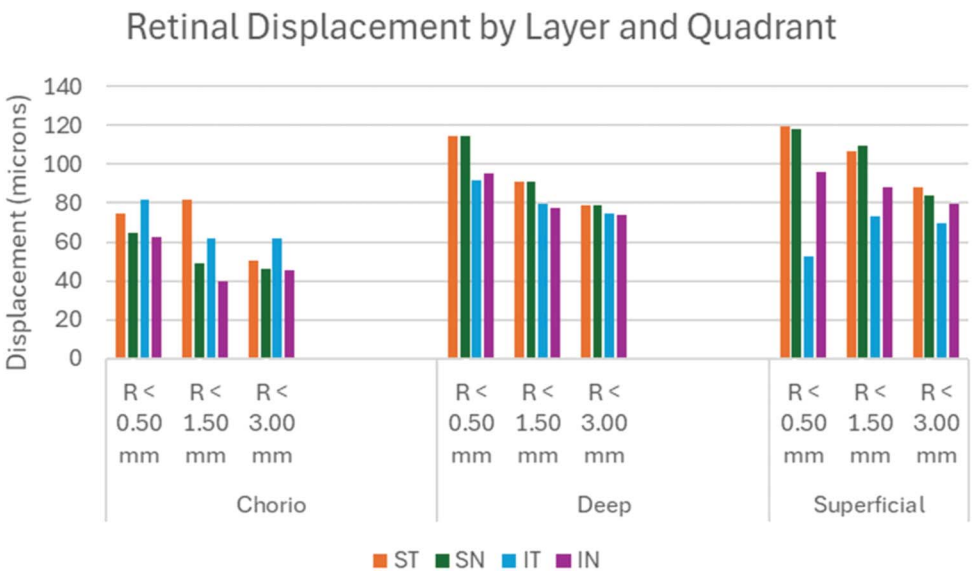

Fig. 3. Retinal plexi displacement by quadrant (ST = SuperoTemporal; SN = SuperNasal; IT = InferoTemporal; IN = InferoNasal) and according to eccentricity: R = radius <0.5 mm, <1.50 mm, and <3 mm.

It should be noted that the ILM is among the stiffest retinal layers,[27,28] a basement membrane without contractile capability per se, whose removal alters the balance of forces between other structures that do retain contractile properties, such as the vessels and the retinal nerve fiber layer, which is rich in microtubules and actin filaments.[29]

The retinal nerve fiber layer, and specifically the interpapillo-macular bundle, also seemed to shape the retinal displacement with limited motion on the nasal side of the MH, invariably oriented along the horizontal meridian, while on the MH temporal side, displacement occurred in a whirl fashion resembling the curving retinal nerve fiber layer path (Figure 6, A–C).

Orientation of ILM peeling during surgery has previously reported to be nonrelevant to retinal displacement: Liu et al[30] found no difference when performed clockwise or counterclockwise in agreement with present series where a single surgeon performed clockwise ILM peeling, with no significant difference in retinal shifting of the single quadrants when right and left eyes were analyzed separately. This finding suggests that the retinal anatomy more than surgeon's peeling direction influences displacement.

Vascular displacement across different layers displayed varying patterns. In most cases (see Figure 7), the deep vascular *plexus* mirrored the behavior of the

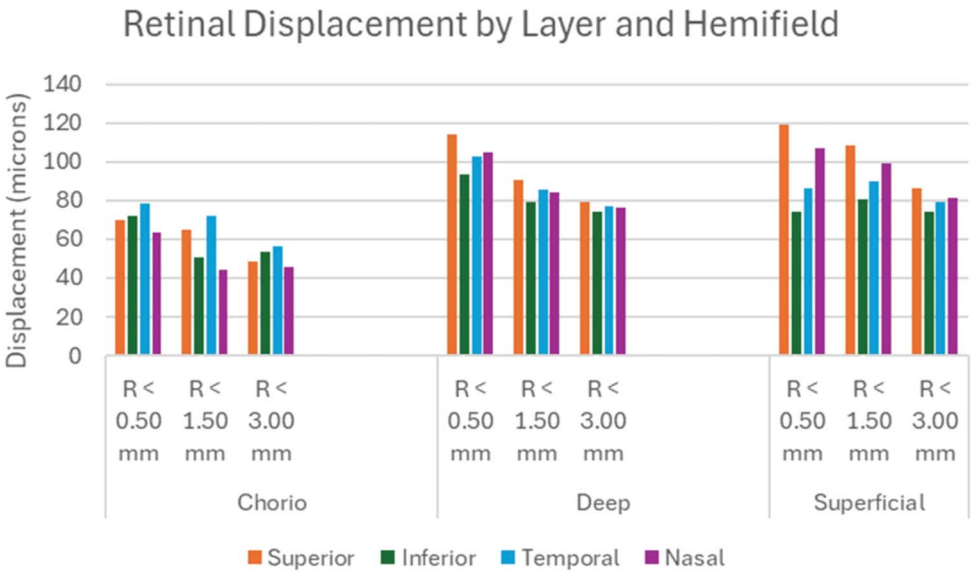

Fig. 4. Retinal plexi displacement by and according to hemifield and eccentricity: R = Radius <0.50 mm, 1.50 mm, and 3.00 mm.

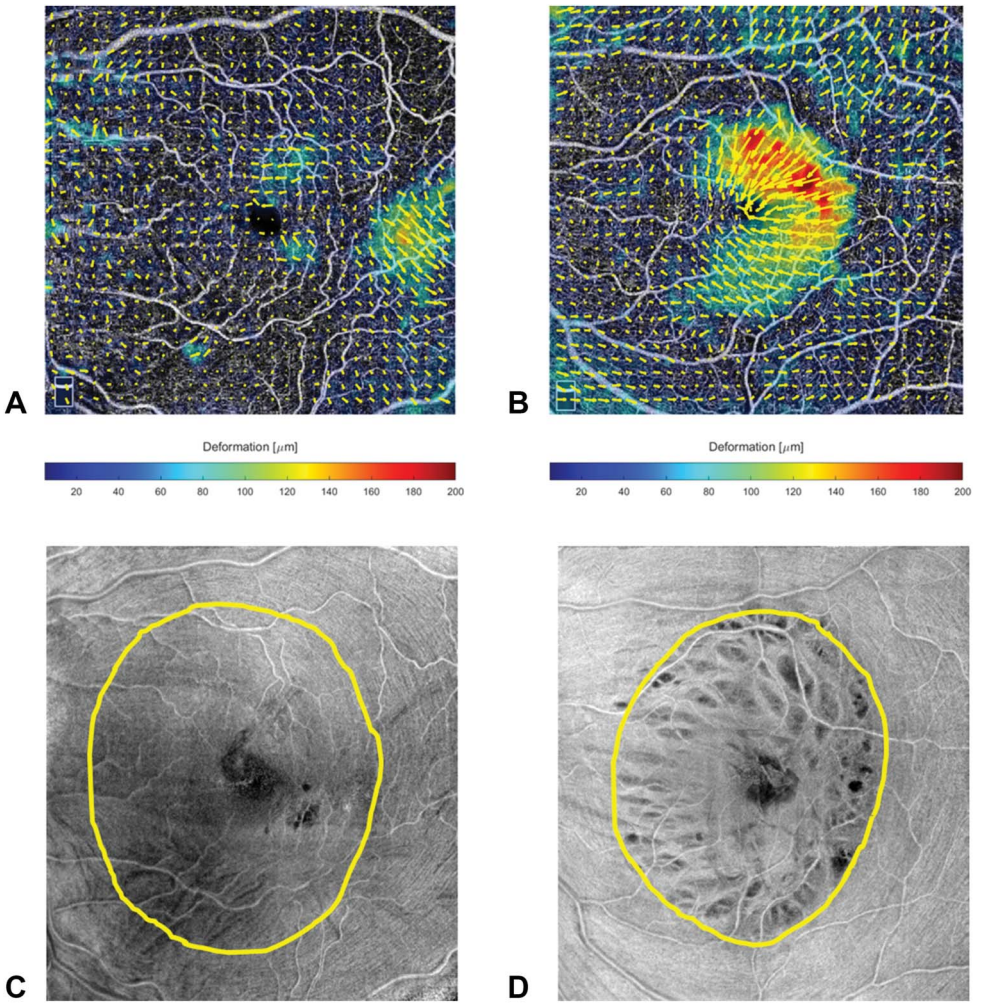

Fig. 5. Retinal displacement vectors (**A** and **B**) and ILM peeling area on en-face OCT images (**C** and **D**) of patients #20 (**A** and **C**) who did not close and pt #4 (**B** and **D**) who did close. Note that the ILM peeling area is comparable while the amount of displacement is very different.

overlying superficial *plexus*, with changes in the choriocapillaris confined to the fovea. However, in others (see Figure 8), the displacement of the deep retina and choriocapillaris was widespread and multifocal. Previous studies noted an increase of choriocapillaris vascular density after MH repair and attributed it to the increased flow and osmolarity from the restored retina.[31] While this explanation accounts for the vascular remodeling observed in the choriocapillaris beneath the MH (Figure 7), it does not fully explain the extensive vascular changes observed in the deep *plexus* and the choriocapillaris present in many patients, as illustrated Figure 8.

The present work suffers the limitations of a relatively small, single surgeon, retrospective series. Furthermore, the image analysis method has only been recently applied to retinal images, and the displacement recognition relies only on the features apparent on the images. On the other hand, the consistency of imaging and clinical data across the follow-up and the analytical measure of retinal shifting using a displacement algorithm through hundreds of points, compared with previous papers using a few anatomical landmarks, represent points of strength. In addition, it should be noted that OCTA images represent the projection of a sphere segment onto a plane, thus "flattening" retinal vessels in a "cartography". This way, the vectorial component lying on the sagittal plane is missed together with the displacement along such plane; we excluded highly myopic eyes to reduce this effect that cannot be eliminated and, in any case, the displacement we measured, lying on the coronal plane, represents a slight underestimation of the 3D displacement.

In summary, our study demonstrated that MH closure is linked to significant retinal displacement of all inquired retinal layers and to remodeling of the choriocapillaris. The surgical peeling removes the ILM constraint, disrupting the balance of forces between the contractile structures surrounding the macula,

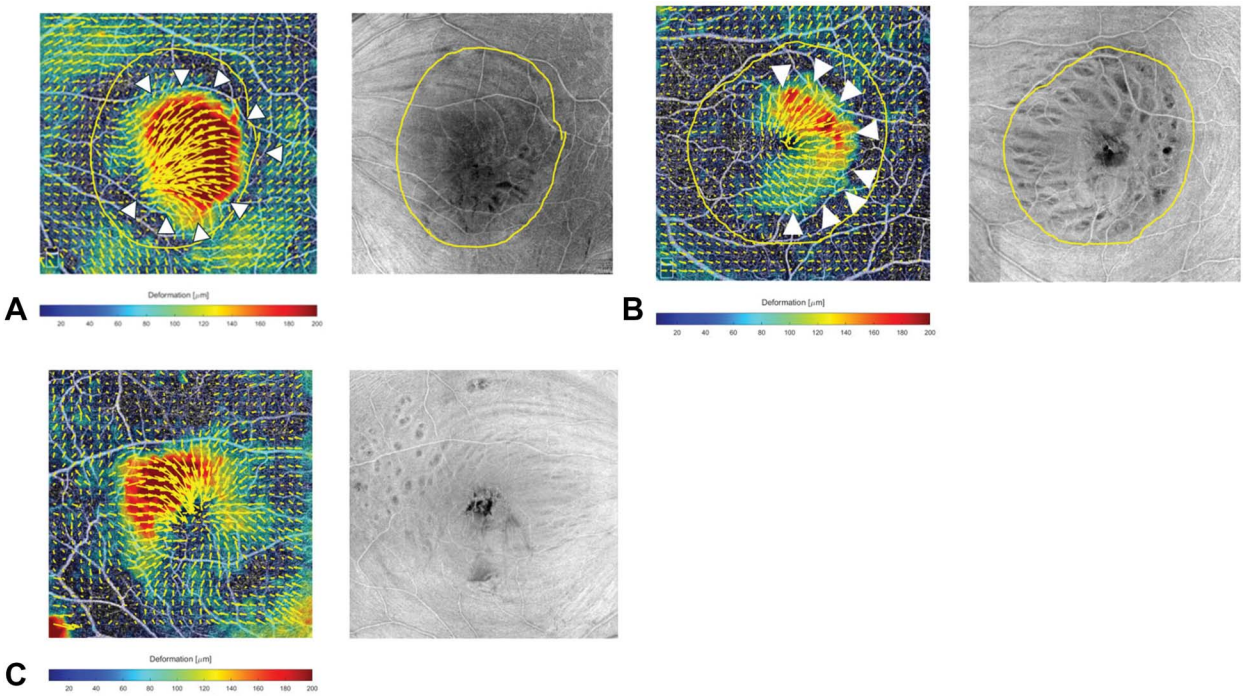

Fig. 6. ILM peeling area compared with superficial retinal displacement between 0 and 6 months of three patients with successfully closed MHs. Note that in all cases, the ILM peeling area (yellow circle) is much wider than the area of maximum retinal displacement, which does not exceed the larger vessels of the superficial retinal plexus (white arrowheads). (c) Note that this patient is one of the few patients showing displacement along the interpapillo-macular bundle and the vectors are precisely oriented along the horizontal meridian.

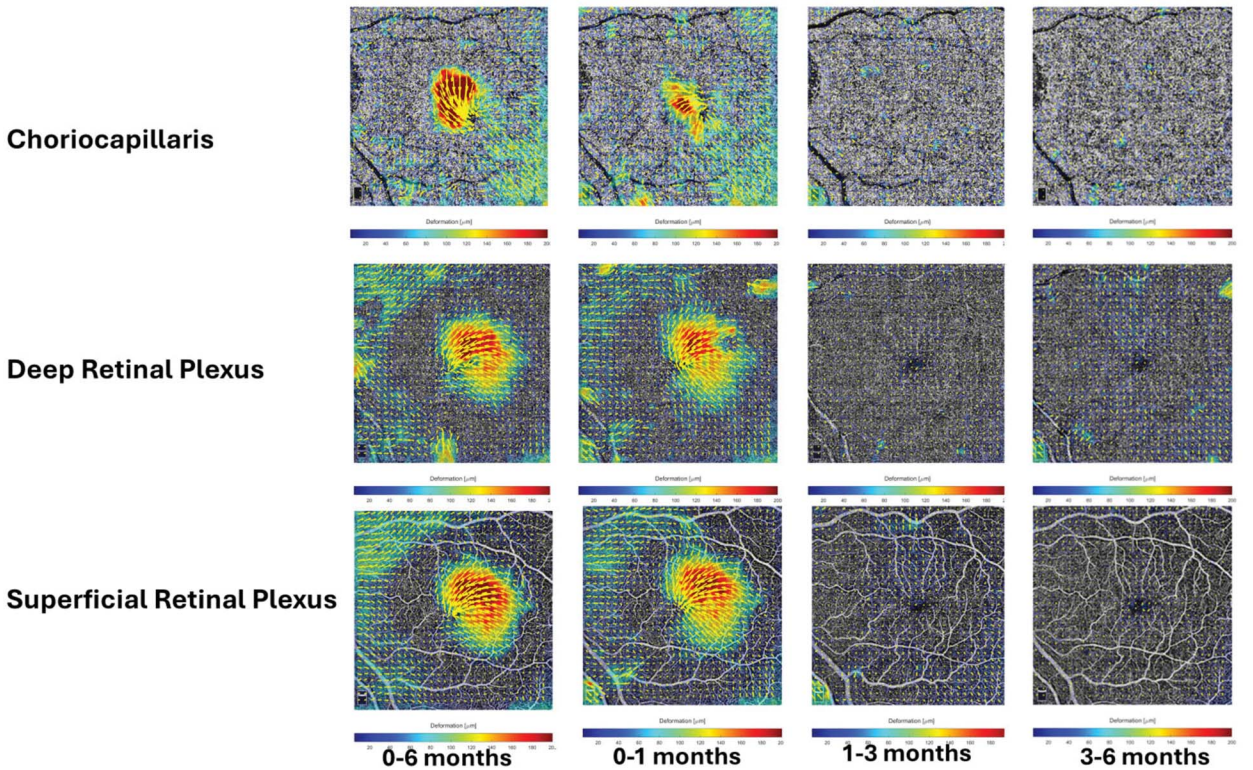

Fig. 7. Patient #26: Vascular displacement across the three plexi during the entire follow-up. Note that displacement occurs entirely within the macular region.

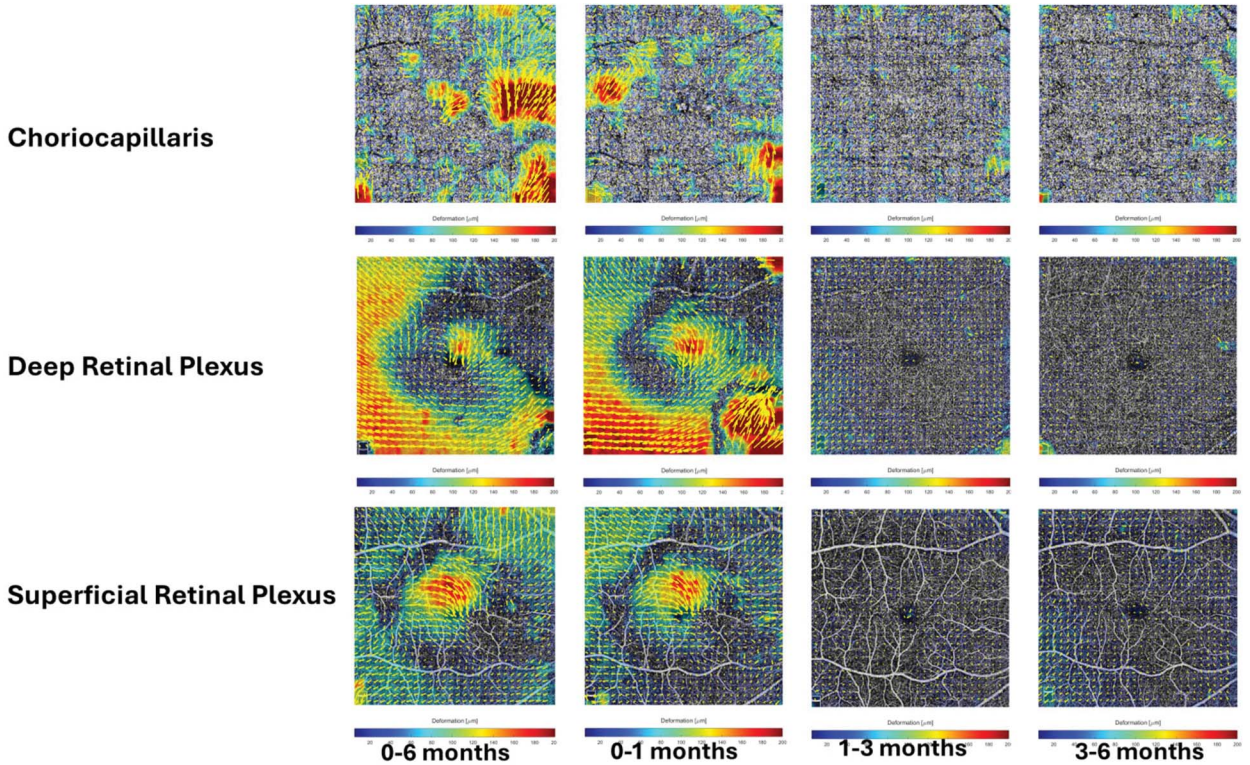

Fig. 8. Patient # 4: Retinal displacement of the superficial plexus is mostly located at the macula while the deep retinal plexus shows a diffuse displacement and the choriocapillaris shows several hot spots of vascular displacement, well outside the foveal region.

including the larger superficial retinal vessels and the densely packed interpapillo-macular bundle of the retinal nerve fiber layer. Notably, the displacement primarily affected the temporal retina and occurred mainly in the early postoperative phase. Further research is needed to clarify the molecular mechanism that triggers and regulate displacement in response to surgery.

Key words: metamorphopsia, macular hole, pars plana vitrectomy, OCT angiography, retinal vascular plexi, retinal displacement.

Acknowledgments

The authors would like to thank the "Fondazione Roma" and the Italian Ministry of Health for financial support. The authors would also like to thank Giuliana Facciolo, Francesca Petruzzella, and Veronica Cherubini for patient study and data gathering.

References

1. Yeh PT, Chen TC, Yang CH, et al. Formation of idiopathic macular hole-reappraisal. Graefes Arch Clin Exp Ophthalmol 2010;248:793–798.
2. Bringmann A, Unterlauft JD, Barth T, et al. Different modes of full-thickness macular hole formation. Exp Eye Res 2021;202:108393.
3. Lee SH, Park KH, Kim JH, et al. Secondary macular hole formation after vitrectomy. Retina 2010;30:1072–1077.
4. Rossi T, Boccassini B, Esposito L, et al. The pathogenesis of retinal damage in blunt eye trauma: finite element modeling. Invest Ophthalmol Vis Sci 2011;52:3994–4002.
5. Ghoraba H, Rittiphairoj T, Akhavanrezayat A, et al. Pars plana vitrectomy with internal limiting membrane flap versus pars plana vitrectomy with conventional internal limiting membrane peeling for large macular hole. Cochrane Database Syst Rev 2023;8:CD015031.
6. Rossi T, Gelso A, Costagliola C, et l. Macular hole closure patterns associated with different internal limiting membrane flap techniques. Graefes Arch Clin Exp Ophthalmol 2017;255:1073–1078.
7. Garg A, Ballios BG, Yan P. Spontaneous closure of an idiopathic full-thickness macular hole: a literature review. J Vitreoretin Dis 2022;6:381–390.
8. Bonińska K, Nawrocki J, Michalewska Z. Mechanism of "flap closure" after the inverted internal limiting membrane flap technique. Retina 2018;38:2184–2189.
9. Rossi T, Trillo C, Schubert HD, et al. Folding the internal limiting membrane flap under perfluorocarbon liquid in large, chronic and myopic macular holes. Graefes Arch Clin Exp Ophthalmol 2019;257:2367–2373.
10. Rossi T, Bacherini D, Caporossi T, et al. Macular hole closure patterns: an updated classification. Graefes Arch Clin Exp Ophthalmol 2020;258:2629–2638.

11. Scarinci F, Querzoli G, Cosimi P, et al. Retinal tectonics after macular pucker surgery: thickness changes and en-face displacement recovery. Retina 2024;44:102–110.
12. Rossi T, Querzoli G, Cosimi P, eet al. Tangential retinal displacement increases after macular pucker surgery: an apparent nonsense. Retina 2024;44:610–617.
13. Spaide RF, Fujimoto JG, Waheed NK, et al. Optical coherence tomography angiography. Prog Retin Eye Res 2018;64:1–55.
14. Arimura E, Matsumoto C, Nomoto H, et al. Correlations between M-CHARTS and PHP findings and subjective perception of metamorphopsia in patients with macular diseases. Invest Ophthalmol Vis Sci 2011;52:128–135.
15. Duker JS, Kaiser PK, Binder S, et al. The International Vitreomacular Traction Study Group classification of vitreomacular adhesion, traction, and macular hole. Ophthalmology 2013; 120:2611–2619.
16. Ahn J, Yoo G, Kim JT, et al. Choriocapillaris layer imaging with swept-source optical coherence tomography angiography in lamellar and full-thickness macular hole. Graefes Arch Clin Exp Ophthalmol 2018;256:11–21.
17. Campbell JP, Zhang M, Hwang TS, et al. Detailed vascular anatomy of the human retina by projection-resolved optical coherence tomography angiography. Sci Rep 2017;7:42201.
18. Hurley JB. Retina metabolism and metabolism in the pigmented epithelium: a busy intersection. Annu Rev Vis Sci 2021;7:665–692.
19. Mihalache A, Huang RS, Patil NS, et al. Pars plana vitrectomy with or without internal limiting membrane peel for macular hole: a systematic review and meta-analysis. Retina 2024;44: 381–391.
20. Wilczyński T, Heinke A, Niedzielska-Krycia A, et al. Optical coherence tomography angiography features in patients with idiopathic full-thickness macular hole, before and after surgical treatment. Clin Interv Aging 2019;14:505–514.
21. Rymer J, Wildsoet CF. The role of the retinal pigment epithelium in eye growth regulation and myopia: a review. Vis Neurosci 2005;22:251–261.
22. Takeyama A, Imamura Y, Fujimoto T, et al. Retinal displacement and intraretinal structural changes after idiopathic macular hole surgery. Jpn J Ophthalmol 2022;66:173–182.
23. Ishida M, Ichikawa Y, Higashida R, et al. Retinal displacement toward optic disc after internal limiting membrane peeling for idiopathic macular hole. Am J Ophthalmol 2014;157:971–977.
24. Chen K, Weiland JD. Anisotropic and inhomogeneous mechanical characteristics of the retina. J Biomech 2010;43: 1417–1421.
25. Qi B, Zhang K, Yang X, et al. Comparison of different internal limiting membrane peeling sizes for idiopathic macular holes: a systematic review and meta-analysis. Ophthalmic Res 2023; 66:1071–1084.
26. Steel DHW, Chen Y, Latimer J, et al. Does internal limiting membrane peeling size matter?. J VitreoRetinal Dis 2017;1:27–33.
27. Henrich PB, Monnier CA, Halfter W, et al. Nanoscale topographic and biomechanical studies of the human internal limiting membrane. Invest Ophthalmol Vis Sci 2012;53:2561–2570.
28. Qu Y, He Y, Zhang Y, et al. Quantified elasticity mapping of retinal layers using synchronized acoustic radiation force optical coherence elastography. Biomed Opt Express 2018;9: 4054–4063.
29. Conde C, Cáceres A. Microtubule assembly, organization and dynamics in axons and dendrites. Nat Rev Neurosci 2009;10: 319–332.
30. Liu J, Hu ZZ, Zheng XH, et al. Displacement of the retina after idiopathic macular hole surgery with different internal limiting membrane peeling patterns. Int J Ophthalmol 2021;14:1408–1412.
31. Nickla DL, Wallman J. The multifunctional choroid. Prog Retin Eye Res 2010;29:144–168.